

Shot noise behavior in single-electron quantum dot-based structures

V. Talbo, S. Galdin-Retailleau, D. Querlioz and P. Dollfus

Institute of Fundamental Electronics, Univ. Paris-Sud, CNRS, UMR 8622, Orsay, France
vincent.talbo@u-psud.fr

Abstract— The 3D Monte Carlo simulation of an Si dot-based double-tunnel junction shows not only the possibility of shot noise suppression down to the Fano factor of 0.5, but also of super-Poissonian noise in the case of multi-state process. The counting statistics of the tunneling events provides a clear interpretation of the different noise regimes according to the balance between the different tunneling rates involved.

Keywords- Double-Tunnel Junction; Shot Noise; Monte Carlo Simulation; Counting Statistics.

I. INTRODUCTION

The analysis of shot noise (SN) and its deviation from the full Poissonian value provides important information on the transport regime in mesoscopic systems and nanodevices [1-8], complementary to that given by the current-voltage characteristics. The SN is characterized by the spectral density of current fluctuations $S(\omega)$ and commonly compared to the spectral density $2e\langle I \rangle$ of a Poissonian process corresponding to a system governed by uncorrelated events, where ω is the frequency, e the elementary charge and $\langle I \rangle$ the average current. The Fano factor, commonly defined at zero frequency as $F = S(0)/2e\langle I \rangle$, is used to measure the possible enhancement (super-Poissonian) and suppression (sub-Poissonian) of SN. Equivalently, the Fano factor may be defined as the ratio $F = \text{var}(N_s)/\langle N_s \rangle$, where N_s is the number of electrons crossing a section of the device during a given time.

Coulomb blockade systems, where the granularity of charge is an essential ingredient, are of strong interest regarding SN. In the case of quantum dots (QDs) coupled to external leads via tunnel junctions, it has been predicted [9] and experimentally observed [4,10] that if the I - V characteristics exhibits well-defined Coulomb staircase, the SN may be suppressed down to the limit $F_{\min} = 1/2$ when the symmetry between in- and out-tunneling rates is achieved. Super-Poissonian SN has been predicted theoretically in metallic systems with multiple dots capacitively coupled [12-15]. It has been also experimentally observed in semiconducting QDs in high bias regime by probing excited states in the dot of long relaxation time [13] and formulated for the general case of nano-objects asymmetrically coupled to the leads giving rise to an NDC regime [3].

Theoretical studies of SN in Coulomb blockade systems are commonly based on one of the two following methods. In the

Korotkov formalism [14] derived in the framework of the "orthodox" approach to single electron transport, a Fourier transform is performed on the master equation to derive a general expression for the spectral density of current fluctuations [12,15]. Alternatively, the method known as the full counting statistics (FCS) [16], consists in the evaluation of the probability distribution functions of the number of electrons transferred to the contacts during a given period of time. It has been used successfully to model the experimental data of time-resolved measurements of electron transport through a quantum dot [13]. However, within these methods, the physical origin of the noise behaviour is often hidden by the mathematical formalism associated with the theory. In this regard, a Monte-Carlo (MC) approach to the time description of tunneling events is a valuable alternative.

In this paper, we analyze the SN behavior of double-tunnel junctions (DTJs) consisting of a silicon QD embedded in silicon oxide and weakly coupled to metallic leads. We focus in particular on the possibility to obtain a super-Poissonian noise in the NDC regime likely to occur in such devices [17]. This theoretical study is based on a Monte Carlo (MC) approach implemented in our simulator SENS (Single Electron Nanostructure Simulation) dedicated to semiconducting QD-based single-electron devices. This time-dependent method of counting statistics simulation is very effective to extract the SN in such devices. The simulation mainly consists in the self-consistent solution of the 3-D Poisson–Schrödinger equations, the calculation of bias-dependent tunneling rates, and the MC treatment of these rates to compute the I - V characteristics and bias-dependent Fano factor.

II. MODEL

The method used in the code SENS to simulate QD-based single-electron devices has been described elsewhere for single- [17,18] and double-dot [19] DTJs or SETs [20]. Here, we just summarize briefly the main stages of the calculation.

The first stage consists in calculating the electronic structure of the QD by solving self-consistently the 3D Poisson and Schrödinger equations within the effective mass and the Hartree approximations which have been proved to be correct for Si NCs of radius greater than 1.5 nm [21,22]. With a view to calculating the tunneling rates, the Hartree method offers the advantage of providing the wave function and the energy level of each electron. The Hamiltonian of each electron includes the confinement potential, the bias potential and the Coulomb potential resulting from the interaction with other electrons [18].

In the second stage, the wave functions are used to calculate the tunneling rates between the dot d and each lead L from the Fermi golden rule, i.e. in the weak coupling limit. The tunneling matrix elements M are given by the Bardeen formula [18,23]

$$M = \frac{\hbar^2}{2m_{barr}} \iint_{S_{barr}} [\psi_L(\vec{r}) \bar{\nabla} \psi_d(\vec{r}) - \psi_d(\vec{r}) \bar{\nabla} \psi_L(\vec{r})] d\vec{S}, \quad (1)$$

where S_{barr} is a surface inside the tunnel barrier which separates arbitrarily the dot and the electrode domains [18], ψ_d and ψ_L are the wave functions in the QD and the lead, respectively, and m_{barr} is the effective mass in the barrier. The wave function ψ_L is deduced from an analytical expression derived within the WKB approximation, which has been proven correct in the simple case of a triangular barrier [18].

Finally, the tunneling rates are used as input data in an MC algorithm to compute the tunnel transitions. It provides the probabilities $P(N)$ of finding N electrons in the dot. The current at the dot-lead interface is finally deduced from

$$I = -e \sum_N P(N) [\Gamma_{dl}(N) - \Gamma_{ld}(N)]. \quad (2)$$

Equivalently, the terminal current at the lead can be determined from the net number N_{sim} of electrons crossing the dot-lead junction in the period of time t_{sim} as

$$I = e N_{sim} / t_{sim}. \quad (3)$$

After repeating the simulation for the same time t_{sim} with different seeds for the random number generator, the statistics of N_{sim} can be extracted and F is simply given by

$$F = \text{var}(N_{sim}) / \langle N_{sim} \rangle. \quad (4)$$

III. RESULTS AND DISCUSSION

We consider the structure schematized in Fig. 1. A 10 nm diameter spherical Si QD is embedded in an SiO_2 matrix which forms tunnel barriers between the dot and the two metallic leads. In such large QD DTJ, the strong influence of bias voltage on the wave functions in the dot and thus on the tunnelling rates is likely to generate an NDC effect and to wash out the expected Coulomb staircase [17]. To make the first two Coulomb staircase steps nearly immune to NDC effect, we designed dissymmetric tunnel barriers, i.e. thicker at the drain side (1.7 nm) than at the source side (1.2 nm).

Though the model is able to take into account the temperature effect through the Fermi distribution of the leads in (3), we have assumed the temperature to be uniformly zero in the device to fully avoid the risk of hiding some important information on the shot noise by the thermal noise. Hence,

though the essential physics is unchanged, the interpretation of SN results will be easier than at finite temperature. In the rest of the paper the subscripts *in* and *out* will be used sometimes in place of subscripts *Sd* and *dD*, respectively.

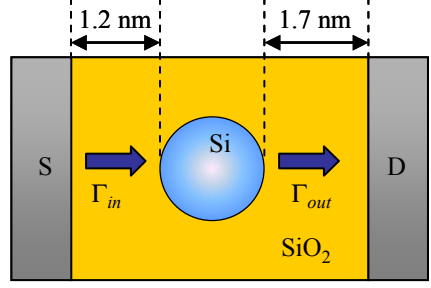


Figure 1. Schematic cross-section of the simulated DTJ with a 10 nm diameter Si QD embedded in SiO_2 . At $T = 0$, the in- and out-tunneling rates are limited to source-to-dot and dot-to-drain processes, respectively.

A. Overall results

The current and the Fano factor are plotted in Fig. 2 as a function of bias voltage. The first and half of the second Coulomb steps are clearly visible in the I - V characteristics. The NDC occurs when increasing further the bias, which transforms the third step in a thin peak and washes out the rest of the staircase. In the first step ($V > 0.3$ V) the SN is sub-Poissonian and F reduces down to 0.66 at $V = 0.59$ V. Then it increases rapidly to become super-Poissonian in the region of the third step. The peak value $F = 3.5$ is reached at $V = 0.72$ V and F decreases continuously to the unity at high bias.

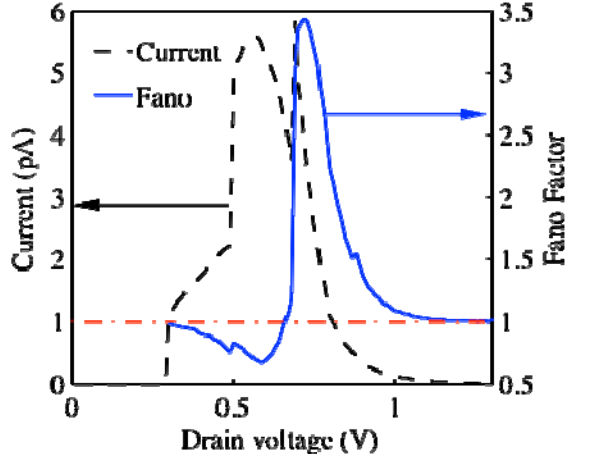


Figure 2. Current (dashed line) and Fano factor obtained from the Korotkov formalism (solid line) and the Monte-Carlo simulation (crosses) as a function of drain voltage. The line $F = 1$ serves as a guide for the eyes.

In Fig. 3, we present the statistical distribution of the number N_{sim} of electrons going through the source junction, during a given time t_{sim} . The statistics is made over 2×10^5 different simulations. The simulated time t_{sim} is chosen here as the time needed for the mean number of electrons to be $\langle N_{sim} \rangle = 50$. The distribution of N_{sim} is plotted for three different bias conditions and compared to the theoretical Poissonian distribution of same average value for N_{sim} . The

comparison of their broadening gives a direct access to the SN regime: it is sub-(super-)Poissonian if the actual distribution is narrower (larger) than the Poissonian distribution. Fig. 3 confirms the results of Fig. 2, i.e. the SN is sub-Poissonian for $V = 0.59$ V, super-Poissonian for $V = 0.72$ V and fully Poissonian for $V = 1.13$ V. However, the origin of the SN suppression and enhancement is still unknown.

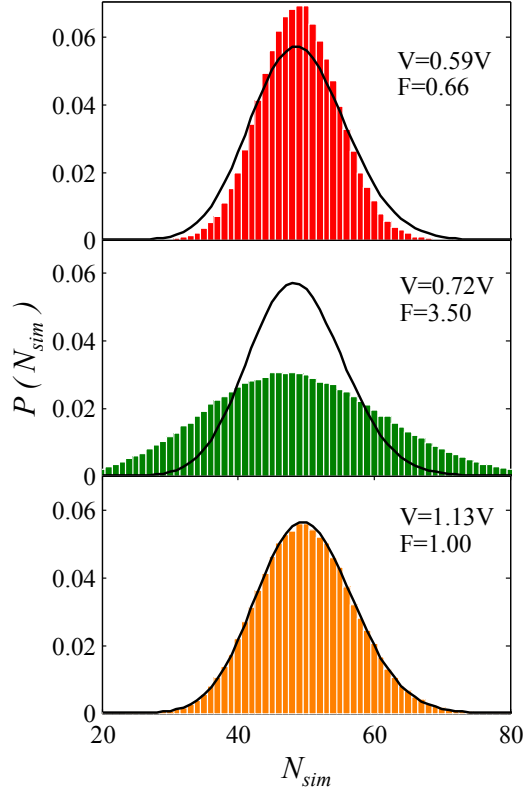


Figure 3. Statistical distribution of the number of electrons crossing junction during a time t_{sim} corresponding to a mean number of 50, for three bias conditions. The statistic has been made over 2×10^5 different simulations (bar chart) and is compared to the Poisson distribution corresponding to 50 electrons and the same current (line).

In the next sub-sections we will elucidate this question from the analysis of tunneling rates in a simplified case with limited possible states. The case of a two-state process is not very interesting since, depending on the symmetry of in- and out-tunneling rates, the SN is either Poissonian if Γ_{in} and Γ_{out} differ strongly or sub-Poissonian otherwise, with the limit value of 0.5 if $\Gamma_{in} = \Gamma_{out}$ [9]. Hence, we will consider the more interesting case of a three-state process where the number of electrons in the dot cannot be higher than 2.

B. The case of a three-state process

The current, the Fano factor and the tunneling rates are plotted in Fig. 4 (a) and (b) for the case of a simulation limited to a three-state process, i.e., for $N \leq 2$. The super-Poissonian noise appears in the second step of the Coulomb staircase, in the NDC regime. The Fano factor reaches the maximum value $F = 1.53$ at $V = 0.76$ V and decreases to 1 at high bias.

To understand the origin of the super-Poissonian noise, we have to keep in mind that compared to a two-state process, the possibility to have two electrons in the dot increases the number of possible transition paths, as illustrated in Fig. 5(a). In a two-state process the only possible sequence for the evolution of N is 0-1-0-1. In the case of a three-state process, there are three possible paths for N_{sim} to reach the value of 2, i.e. "0-1-0-1", "1-2-1-2", or "0-1-2". The character of SN is then fully determined by the relative probabilities of these paths, as explained below. The number of occurrences of these paths is summarized in Table 1 for three situations of sub-Poissonian, super-Poissonian and Poissonian noise, respectively, for a time duration corresponding to 500,000 tunneling events.

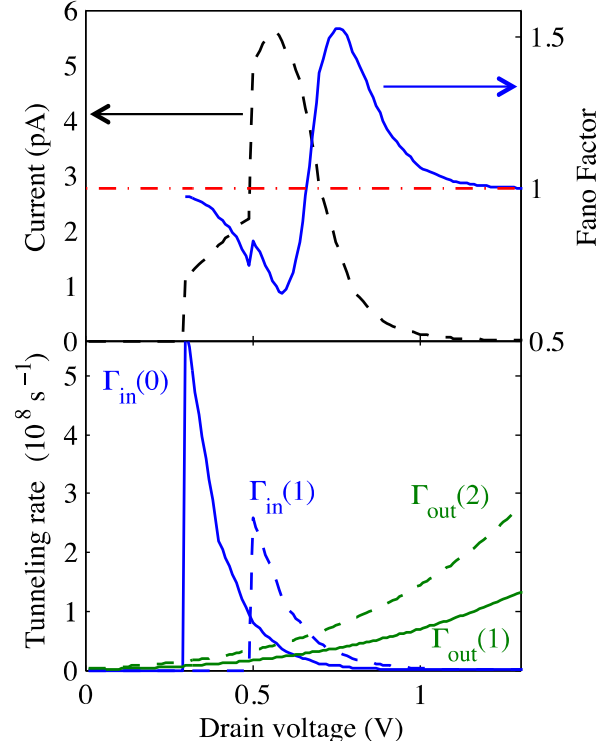


Figure 4. (top) Current-voltage characteristics (dashed line) and Fano factor (solid) for a 3-state process and (bottom) the corresponding tunneling rates.

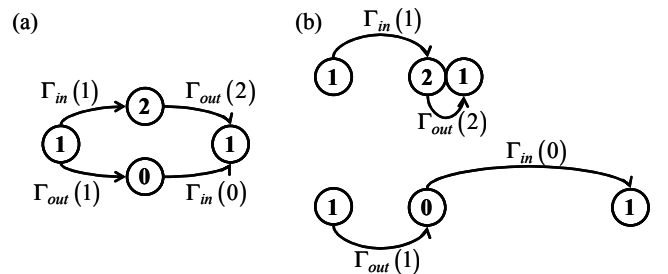


Figure 5. Schematic description of (a) all possible transitions and (b) of the transitions in the particular case leading to a super-Poissonian noise with $\Gamma_{in}(1) = \Gamma_{out}(1)$ and $\Gamma_{in}(0) \gg \Gamma_{out}(2)$.

TABLE I. Number of occurrences of the different paths (or sequences of N) for three bias conditions. The statistics are made over a total of 500,000 tunneling events through the source barrier.

| | | Number of events per sequence of N | | |
|------|------|--------------------------------------|---------------|----------------|
| V | F | 0-1-0-1 | 0-1-2 | 1-2-1-2 |
| 0.59 | 0.66 | 6343 (2.9%) | 33311 (15.4%) | 177033 (81.7%) |
| 0.76 | 1.53 | 81416 (43.1%) | 61074 (32.3%) | 46435 (24.6%) |
| 1.3 | 1.00 | 248965 (99.8%) | 516 (0.2%) | 1 (0%) |

At the minimum of noise ($V = 0.59$ V, $F = 0.66$), we have $\Gamma_{in}(1) \gg \Gamma_{out}(1)$ and thus the path 1-2-1-2 dominates. Since $\Gamma_{in}(1) \approx \Gamma_{out}(2)$, the situation is similar to that of the 2-state process, with a sub-Poissonian noise. For the maximum of SN ($V = 0.76$ V, $F = 1.53$), we have $\Gamma_{in}(1) \approx \Gamma_{out}(1)$ and there is no dominant path, as confirmed in Table 1, though the path 1-0-1-0 is a bit more frequent. Moreover, since $\Gamma_{out}(2) \gg \Gamma_{in}(0)$, the average durations of the different paths are different, as illustrated in Fig. 5(b), which broadens the variance of N and yields a super-Poissonian SN. It should be noted that F_{max} is not reached here when $\Gamma_{in}(1) = \Gamma_{out}(1)$, because in this case the condition $\Gamma_{out}(2) \gg \Gamma_{in}(0)$ is not met. The character of SN is thus governed by a fragile balance between the different tunneling rates. The situation is much more clear at high bias ($V = 1.3$ V, $F = 1$) where we have $\Gamma_{in}(1) \ll \Gamma_{out}(1)$ and $\Gamma_{in}(0) \ll \Gamma_{out}(1)$, which is exactly the same configuration as for the fully Poissonian noise in the two-state process.

IV. CONCLUSION

The 3D self-consistent MC simulation of a semiconducting DTJ allowed us to extract the counting statistics of tunneling events and to show the possibility of shot noise enhancement. The detailed analysis of tunneling rates and of the evolution of the number of electrons in the dot made it possible to clarify the conditions of the different SN regimes. In particular the super-Poissonian noise results from a subtle balance between the different bias-dependent tunneling rates in the case of a multi-state process.

REFERENCES

- [1] Th. Martin and R. Landauer, "Wave-packet approach to noise in multichannel mesoscopic systems," Phys. Rev. B, vol. 45, pp. 1742-1755, 1992
- [2] Ya. M. Blanter, M. Büttiker, "Shot noise in mesoscopic conductors," Phys. Rep., vol. 336, pp. 1-166, 2000.
- [3] A. Thielmann, M. H. Hettler, J. König and G. Schön, "Super-Poissonian noise, negative differential conductance, and relaxation effects in transport through molecules, quantum dots, and nanotubes," Phys. Rev. B, vol. 71, p. 045341, 2005.
- [4] T. Choi, T. Ihn, S. Schön and K. Ensslin, "Counting statistics in an InAs nanowire quantum dot with a vertically coupled charge detector," Appl. Phys. Lett., vol. 100, p. 072110, 2012.
- [5] S. S. Safonov et al., "Enhanced Shot Noise in Resonant Tunneling via Interacting Localized States," Phys. Rev. Lett., vol. 91, P. 136801, 2003.
- [6] G. Iannaccone, M. Macucci and B. Pellegrini, "Shot noise in resonant-tunneling structures," Phys. Rev. B, vol. 55, pp. 4539-4550, 1997.
- [7] X. Oriols, A. Trois and G. Blouin, "Self-consistent simulation of quantum shot noise in nanoscale electron devices," Appl. Phys. Lett., vol. 85, pp. 3596-3598, 2004.
- [8] V. Nam Do, P. Dollfus and V. Lien Nguyen, "Transport and noise in resonant tunneling diode using self-consistent Green function calculation," J. Appl. Phys., vol. 100, p. 093705, 2006.
- [9] S. Hershfield, J. H. Davies, P. Hyldgaard, C. J. Stanton and J. W. Wilkins, "Zero-frequency current noise for the double-tunnel-junction Coulomb blockade," Phys. Rev. B, vol. 47, pp. 1967-1979, 1993.
- [10] H. Birk, M. J. M. de Jong and C. Schönenberger, "Shot-Noise Suppression in the Single-Electron Tunneling Regime," Phys. Rev. Lett., vol. 75, pp. 1610-1613, 1995.
- [11] M. Gattobigio, G. Iannaccone and M. Macucci, "Enhancement and suppression of shot noise in capacitively coupled metallic double dots," Phys. Rev. B, vol. 65, p. 115337, 2002.
- [12] V. Hung Nguyen, V. Lien Nguyen and P. Dollfus, "Shot noise in metallic double dot structures with negative differential conductance," Appl. Phys. Lett., vol. 87, p. 123107, 2005.
- [13] S. Gustavsson et al., "Counting statistics and super-Poissonian noise in a quantum dot: Time-resolved measurements of electron transport," Phys. Rev. B, vol. 74, p. 195305, 2006.
- [14] A. N. Korotkov, "Intrinsic noise of the single-electron transistor," Phys. Rev. B, vol. 49, pp. 10381-10392, 1994.
- [15] D. Sánchez, "Magnetoasymmetric current fluctuations of single-electron tunneling," Phys. Rev. B, vol. 79, p. 045305, 2009.
- [16] L. S. Levitov, H.-W. Lee, and G. B. Lesovik, "Electron counting statistics and coherent states of electric current," J. Math. Phys., vol. 37, pp. 4845-4866, 1996.
- [17] J. Sée, P. Dollfus and S. Galdin-Retailleau, "Theoretical investigation of negative differential conductance regime of silicon nanocrystal single-electron devices," IEEE Trans. Electron Devices, vol. 53, pp. 1268-1273, (2006).
- [18] J. Sée, P. Dollfus, S. Galdin-Retailleau and P. Hesto, "From wavefunctions to current-voltage characteristics: overview of a Coulomb blockade device simulator using fundamental physical parameter," J. Comput. Electron., vol. 5, pp. 35-48, 2006.
- [19] A. Valentin, S. Galdin-Retailleau and P. Dollfus, "Phonon effect on single electron transport in two-dot semiconductor devices," J. Appl. Phys., vol. 106, p. 044501, 2009.
- [20] V. Talbo, A. Valentin, S. Galdin-Retailleau and P. Dollfus, "Physical simulation of Silicon nanocrystal-based single-electron transistors," IEEE Trans. Electron Dev., vol. 58, pp. 3286-3293, 2011.
- [21] J. Sée, P. Dollfus and S. Galdin, "Comparison of a density functional theory and a Hartree treatment of silicon quantum dot," J. Appl. Phys., vol. 92, pp. 3141-3146, 2002.
- [22] J. Sée, P. Dollfus and S. Galdin, "Comparison between a sp^3d^5 tight-binding and an effective-mass description of silicon quantum dots," Phys. Rev. B, vol. 66, p. 193307, 2002.
- [23] J. Bardeen J. Tunnelling from a many-particle point of view, Phys. Rev. Lett., vol. 6, pp. 57-59, 1961.